Eur. Phys. J. B **5**, 37–43 (1998)

THE EUROPEAN PHYSICAL JOURNAL B

Magnetization dynamics below T_c of EuO and EuS*

Evidences for effects of dipolar-anisotropic fluctuations

D. Görlitz[a] and J. Kötzler

Institut für Angewandte Physik und Zentrum für Mikrostrukturforschung, Jungiusstr.11, 20355 Hamburg, Germany

Received: 4 March 1998 / Accepted: 12 May 1998

Abstract. Between 4.2 K and the Curie temperatures of the cubic Heisenberg ferromagnets EuS and EuO, their homogeneous dynamic susceptibilities $\chi_{zz}(\omega, T, H)$ have been investigated by means of a broadband reflectometer operating from 0.1 GHz to 40 GHz. For internal magnetic fields larger than the anisotropy fields $H_A(T)$ of both materials, their static susceptibilities $\chi_z(T, H)$ exhibit a $1/\sqrt{H}$-divergence, which reveals *quantitatively* the dominance of dipolar-anisotropic spin-wave fluctuations. $\chi_{zz}(\omega)$ displays a Lorentzian shape the damping frequency of which obeys scaling in terms of $\chi_z(T, H)$. The scaling function agrees quantitatively with work by Frey and Schwabl [19] for dipolar Heisenberg ferromagnets at temperatures *above* T_c. Building upon their approach, the resonance frequency of the Lorentzian can be related to a memory effect in the damping determined by the large value of the relaxation rate of the longitudinal magnetization fluctuations Γ_ℓ. For EuS, this relation is substantiated directly by inelastic neutron scattering. All these features reveal the hitherto uncovered importance of the dipolar anisotropic fluctuations below T_c of ferromagnets.

PACS. 75.30.Cr Saturation moments and magnetic susceptibilities – 75.40.Cx Static properties – 75.40.Gb Dynamic properties

1 Introduction

Above the Curie temperature, the dynamics of the homogeneous magnetization of Heisenberg ferromagnets has been investigated experimentally as well as theoretically in great detail and is regarded now as to be well understood. In particular, the importance of the influence of the dipolar anisotropic fluctuations on the critical dynamic behavior has been demonstrated for the $q = 0$-suceptibility [1–13] of EuS and EuO and by neutron scattering on Fe [13,14], EuO [15,16] and EuS [17,18]. Along with recent theoretical work based on the mode coupling (MC) approach [19,20] these results led to an almost complete description of the important effect of the inevitable long-range dipole-dipole interaction on the magnetization dynamics at large wavelengths, including the homogeneous limit.

At very low temperatures, $T \ll T_c$, the dynamics result from magnetization rotations while for elevated temperatures *below* T_c, where thermal fluctuations enter, detailed experimental investigations of the homogeneous dynamics in model Heisenberg ferromagnets do not exist. Recently, a clear signature of dipolar-anisotropic fluctuations has been detected in the static susceptibility $\chi_z(T, H)$ of EuS [21] not only in the classical spin-wave regime [22,23] but also at temperatures surprisingly close to the Curie point.

Here we report the first systematic investigations of the temperature and field dependence of the *dynamic* susceptibility $\chi_{zz}(\omega)$ on single-crystalline spheroids of the cubic ferromagnets EuS ($T_c = 16.5$ K) and EuO ($T_c = 69.5$ K) below their Curie temperatures. Due to their strongly localized moments and low anisotropy fields, these materials are regarded as very good realizations for Heisenberg ferromagnets. The large moments of the Eu^{2+} ions of $7\mu_B$ and their high density in the NaCl-structure pronounce the dipole-dipole interactions and suggest to study their effects also below T_c.

In Section 2 we describe our experimental microwave setup for measuring the frequency, temperature and field variation of $\chi_{zz}(\omega; T, H)$ between 0.1 GHz and 40 GHz. Results of frequency scans typical for EuS and EuO are presented, which reveal for $\chi_{zz}(\omega)$ heavily damped Lorentzian shapes. We examine here the domain-free state and to this end we consider finite internal magnetic fields $H = H_{ext} - N_z \cdot M_z > 0$, where all domain walls are expelled from the sample. In Section 3 we investigate the effects of thermal fluctuations and in particular of the dipolar anisotropy on the *static* susceptibility. This is followed by analyses of the shape of $\chi_{zz}(\omega)$ and of the dynamic parameters, *i.e.* resonance frequencies and linewidths, in Section 4. These results are discussed in Section 5 in the light of the MC approach of Frey and Schwabl [19,20] and in terms of very recent results from inelastic scattering of polarized neutrons [18,24].

* Dedicated to Professor F. Schwabl at his 60th birthday

[a] e-mail: goerlitz@physnet.uni-hamburg.de

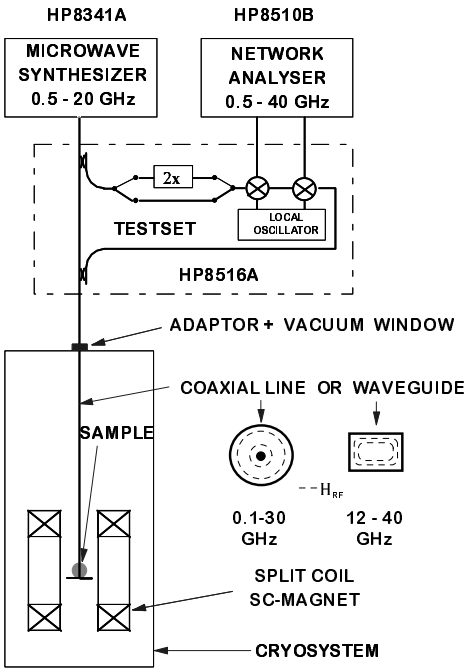

Fig. 1. Layout of the microwave reflectometer for $\chi(\omega)$-measurements between 0.1 GHz and 40 GHz.

2 Experiment

For the measurements we used an upgraded version of a broad-band, vectorial microwave reflectometer described previously [25]. In this setup, sketched in Figure 1, the sample is placed in the maximum of the microwave magnetic field at the shortened end of a microwave transmission line. This allows for both principal orientations of the rf-field with respect to the static magnetic field provided by a superconducting split-coil magnet. In this work the 'parallel' orientation is employed, where H_{RF} directly couples to magnetization fluctuations parallel to the field.

The microwave amplitude is supplied by a synthesizer sweeper (HP8341A) feeeding a home-made coaxial transmission line at frequencies between 0.1 GHz and 30 GHz. High quality waveguides are used above 12 GHz. A coaxial adaptor containing a vacuum tight window couples the sample insert to the test-set (HP8516A) of a vector network analyzer (HP8510B). This records continuously the complex reflection coefficient of the sample, $R(f) = R'(f) - i\ R''(f)$, between $f = 0.1$ GHz and 40 GHz. As shown in reference [25] the dynamic susceptibility $\chi(f) = \chi'(f) - i\ \chi''(f)$ can be deduced from the normalized reflection coefficient $r \equiv R/R_0$ where R_0 denotes the signal at $\chi = 0$ reached at sufficiently large fields:

$$\chi'(f) = \frac{1}{\eta f} \quad \frac{1 - r^{'2} - r^{''2}}{(1+r')^2 + r^{''2}}, \tag{1}$$

$$\chi''(f) = \frac{1}{\eta f} \quad \frac{2r''}{(1+r')^2 + r^{''2}}. \tag{2}$$

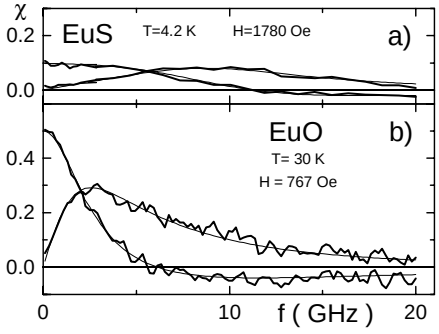

Fig. 2. Absorption and dispersion of (a) an EuS sphere at $T = 4.2$ K for the internal field $H = 1780$ Oe and (b) an EuO sphere $T = 30$ K for $H = 767$ Oe. Solid lines correspond to single Lorentzian model, equation (3).

The filling factors η of the samples in the coaxial line were determined by measuring $\chi(f)$ in a calibration $\lambda/4$-cavity of same geometry and sample location operating at 1.9 GHz [3]. For the rectangular waveguide, a $\lambda/2$-waveguide-cavity operating at 9 GHz was used. In both assemblies the rf-amplitude across the sample was kept constant so that the filling factors remained independent of frequency. The calibrations were checked by comparing the low frequency results for $\chi(\omega)$ of EuS at T_c to the data from reference [7].

The sample insert is housed by a double-walled tube immersed in the liquid Helium bath which cools also the superconducting magnet. By means of a temperature sensor (Lake Shore Cryogenics, Cernox CX-series) and an ohmic heater, both connected to a PID temperature controller (Lake Shore Cryogenics, model DRC-91), the sample temperatures between 4.2 K and 150 K could be stabilized in external magnetic fields up to 18 kOe.

As an example, Figure 2 shows two frequency scans obtained on 3 mm crystalline spheres of EuS and EuO in internal magnetic fields $H \equiv H_{ext} - N_z M_z > H_A(T)$ [26]. Here the coaxial transmission line was used up to 18 GHz. As a prominent feature one realizes the change of the sign in the dispersion signals near 12 GHz in EuS and 7 GHz in EuO, respectively, which is accompanied by a broad maximum in the absorption. Both features can be well fitted by a single, heavily damped Lorentzian:

$$\chi_{zz}(\omega) = [\chi_z^{-1}(0) + \frac{i\omega}{L_z} - \frac{\omega^2}{\Omega_z^2} + N_z]^{-1}. \tag{3}$$

where $N_z = 1/3$ provides the demagnetization correction [27]. The fits are indicated by full lines in Figure 2. $L_z(T,H)$ represents the kinetic coeffient associated with the intrinsic damping and $\Omega_z(T,H)$ denotes an intrinsic resonance frequency determining the zero of the dispersion. These two parameters contain the essential information on the linear magnetization dynamics and will be discussed in Section 4.

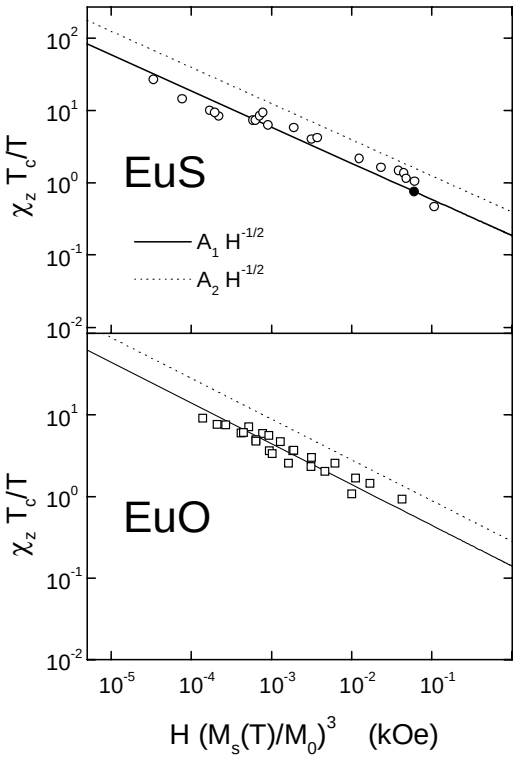

Fig. 3. Goldstone divergence of the static susceptibilities $\chi_z(0)(\circ\square)$ and $\chi_z(q_t)(\bullet)$ of (a) EuS and (b) EuO at small internal fields, $H \ll M_s$. Both are compared for dipolar anisotropic (A_1) and Heisenberg-type (A_2) fluctuations, respectively (Eq. (3)).

3 Static susceptibilities

The static susceptibilities $\chi_z(0)$ obtained from the fits of $\chi_{zz}(\omega)$ to equation (3) at magnetic fields $H_A(T) < H \ll M_s(T)$ are shown in Figure 3 for temperatures 4.2 K $< T \leq T_c$. In order to elucidate the predicted effect of the spin-wave fluctuations [22,23], the susceptibility is normalized by the thermal factor T/T_c and plotted on a double-logarithmic scale *versus* the internal field weighted by the third power of the reduced spontaneous magnetization, ($M_0 = M_s(0)$). For all temperatures, the data for both ferromagnets fall on common power laws, which decrease with $H^{-1/2}$.

This divergence of the parallel susceptibility at small field H has been predicted at first by Holstein and Primakoff [22] within the spin-wave theory for Heisenberg ferromagnets and was confirmed thereafter by many others (*e.g.* Refs. [23,28–33]). Based on general hydrodynamic arguments for ferromagnets with Heisenberg exchange, Prokrovsky [23] demonstrated that the anisotropic dipolar interaction leaves only the correlation between the modes perpendicular to both $\mathbf{M}$ *and* $\mathbf{q}$ (Goldstone-like mode δS^G_{SW} see Fig. 4b) critical, while the correlations between the modes in the $(\mathbf{M},\mathbf{q})$-plane remain finite. As

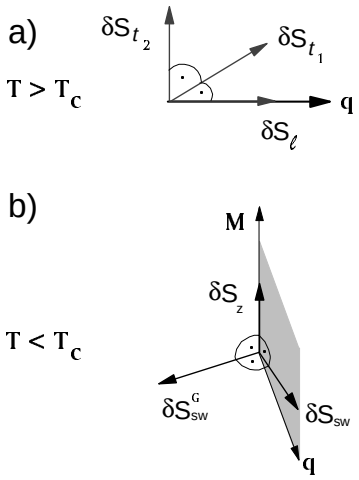

Fig. 4. Magnetization modes classified with respect to (a) the wave vector $\mathbf{q}$ above T_c and (b) to the spontaneous magnetization $\mathbf{M}_s$ below T_c.

a consequence, the amplitude A_n of the parallel susceptibility [21],

$$\chi_z^{sw}(T, H \ll M_s) = A_n \quad \frac{T}{T_c}\left(\frac{M_0}{M_s}\right)^{3/2} \frac{1}{H^{1/2}}, \qquad (4)$$

$$A_n = \frac{n}{16\pi}\, q_d^3\, \frac{k_B\, T_c}{\mu_0 M_0^{3/2}}, \qquad (5)$$

is reduced by the dipolar interaction, because the number n of Goldstone modes is lowered from the Heisenberg value $n = 3 - 1 = 2$ to the dipolar one, $n = 1$. Inserting the dipolar wavenumbers $q_d = 0.24$ Å^{-1} and $q_d = 0.15$ Å^{-1} extracted from neutron scattering experiments on EuS [34] and from $\chi_z(0)$-data above T_c for EuO [6], the solid lines in Figure 3 are obtained. Obviously, the dipolar-reduced amplitudes A_1 describe the data much better than the isotropic values A_2.

4 Scaling of damping and resonance frequencies

At first, we address ourselves to the kinetic coefficient for the damping, $L_z(T,H)$ which increases either by lowering the field at fixed temperatures, $T < T_c$, or by raising the temperature at a low field. This socalled critical speeding up when approaching T_c from *below* very much resembles the behavior of L_z observed *above* T_c [6]. Therefore, it is suggestive to examine whether the scaling behavior of L_z, evidenced in the paramagnetic critical state [7], also holds in the ferromagnetic phase. In Figure 5, for this purpose, we plot the measured kinetic coefficients as a function of the static susceptibilities for both materials. In fact, a rather convincing scaling is obtained, which extends down to temperatures as low as 0.25 T_c in EuS and to 0.72 T_c in EuO. We note that this scaling holds only for internal fields larger than the anisotropy fields $H_A(T)$ of

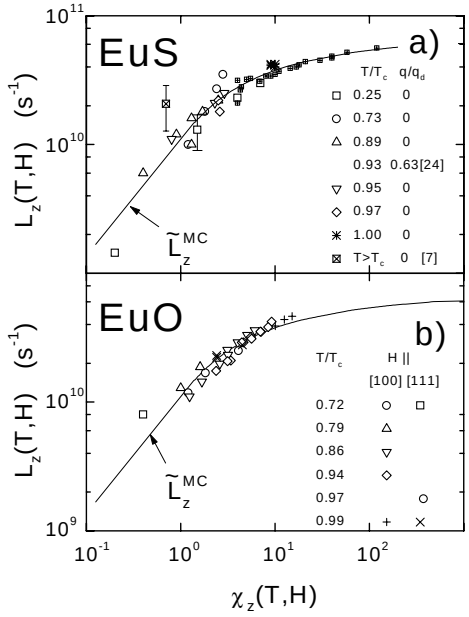

Fig. 5. Scaling representation of the kinetic coefficient L_z of the damping of the homogeneous magnetization dynamics in fields above the anisotropy fields: (a) EuS and (b) EuO. Solid lines represent $\tilde{L}_z(\omega = 0)$ calculated from equation (12).

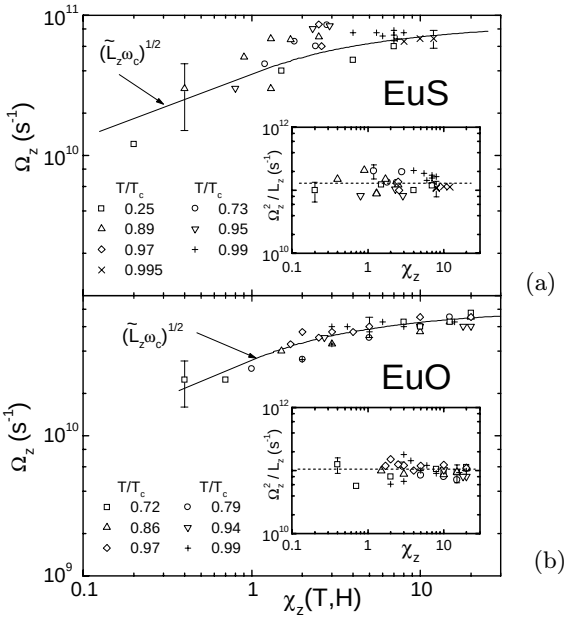

Fig. 6. Scaling representation of the resonance frequency Ω_z of the homogeneous susceptibility defined in equation (2): (a) EuS and (b) EuO. Solid curves were calculated using the MC-result $L_z(\chi_z)$ (Fig. 5) and the correlation frequencies, $\omega_c = \Omega_z^2/L_z$ (see insets).

EuO [35] and EuS [36]. Furthermore, the data of the more anisotropic EuO fall on the same scaling function for both orientations, $H||[100]$ and $H||[111]$, which, therefore, can be considered to reflect the isotropic magnetic behavior.

It is common sense to associate scaling behavior near T_c with the fact that the magnetic response functions scale with the diverging correlation length $\xi(T,H)$ of the order parameter, $\mathbf{M_s} = M_s\mathbf{e_z}$. Among them is the static susceptibility, $\chi_z(T,H) = (q_d\,\xi(T,H))^2$ [7], which may thus be used to explore the scaling regime. Approaching T_c from above, the critical speeding-up of L_z results from a reduction of the Anderson-Weiss exchange narrowing due to the growth of the spin-correlations [37,38]. This speeding-up saturates when the dipolar anisotropy begins to dominate the spatial correlations between the magnetization fluctuations. This socalled *static* dipolar crossover has been observed directly by polarized neutron scattering [34]. In the limit of low frequencies, $\omega \leq L_z/\chi_z$ [6], the *dynamical* crossover for the kinetic coefficient could quantitatively be described by numerical mode coupling (MC) results derived for *unmagnetized* dipolar Heisenberg ferromagnets, *i.e.* for $T \geq T_c, H = 0$ [19]. In Figure 5, the predicted $\tilde{L}_z(\omega \to 0;\ \chi_z(T,H))$ is fitted to the data using the values at criticality, $L_z(T_c, H = 0)$, as the only parameters. Their numbers have been explained along with those for several other Heisenberg ferromagnets in reference [6]. As the most interesting feature of Figure 5 we note, that the scaling function in the ordered state agrees excellently with $\tilde{L}_z(0,\chi_z)$ despite the fact that this function was derived for $T > T_c$ and for zero field. We discuss this point in Section 5.

The scaling property of the second dynamic parameter, *i.e.* of the resonance frequency $\Omega_z(T,H)$, is illustrated in Figure 6. At a first glance, the appearance of a resonance in the dynamics of fluctuations δS_z parallel to the magnetization is puzzling, since in the homogeneously magnetized state a torque acting on δS_z does not exist. One rather expects a simple Debye-behavior, $\chi_{zz}(\omega) = [\chi_z^{-1}(T,H) + i\omega/\tilde{L}_z + N_z]^{-1}$. However, this can explain the experimentally observed Lorentzian, equation (3), only if the kinetic coefficient displays the following frequency dependence:

$$\tilde{L}_z(\omega;T,H) = \frac{L_z(T,H)}{1 + i\omega Ł_z(T,H)/\Omega_z^2(T,H)}\,. \qquad (6)$$

This socalled memory of the kinetic coefficient becomes important for frequencies larger than a characteristic frequency, $\Omega_z^2/L_z \equiv \omega_c$. A central result emerging from this homogeneous magnetization dynamics is that ω_c does neither depend on the temperature nor on the magnetic field. According to the insets to Figure 6, one finds $\omega_c = 1.2(4) \times 10^{11}$ s^{-1} and $\omega_c = 1.0(3) \times 10^{11}$ s^{-1} for EuS and EuO, respectively. Adopting these values for ω_c and using the MC-curves $\tilde{L}_z(0,\chi_z)$ displayed in Figure 5, it is then possible to describe the scaling functions, $\Omega_z(T,H) = \Omega_z(\chi_z(T,H))$, within the experimental error margins for both EuS and EuO.

5 Discussion

At the outset, we recall the exact expression for the Onsager kinetic coefficient of the magnetization as determined *e.g.* by the linear response theory [20,37],

$$\tilde{L}_z(\omega) = \int_0^\infty dt(\dot{S}_z(t)\dot{S}_z(0))e^{i\omega t}. \qquad (7)$$

Accordingly, the damping results from the correlation between the torques, $\dot{S}_z = (i/\hbar)[\mathcal{H}, S_z]$, acting on the total spin. In concentrated ferromagnets, the torque is governed by the dipolar interaction between the moments [11], so that the spin-lattice interaction can be ignored, $\mathcal{H}_{s\ell} \ll \mathcal{H}_{dd}$.

For this socalled dipolar Heisenberg ferromagnet $\tilde{L}_z(\omega)$ has been evaluated by many authors [20,37–39] within the random phase approximation (RPA) at zero field for temperatures *above* T_c. There, in the absence of a finite magnetization, the fluctuations are classified with respect to their propagation vectors $\mathbf{q}$ (see Fig. 4a) into one longitudinal ($\delta\mathbf{S} \parallel \mathbf{q}$) and two transverse ($\delta\mathbf{S}\perp\mathbf{q}$) modes. Within the RPA they decouple to give

$$\tilde{L}_z^{MC}(\omega) = \Omega_d^2 \sum_{\mathbf{q}} \int_0^\infty dt\ C_\ell(\mathbf{q},t)C_t(\mathbf{q},t)e^{i\omega t}, \qquad (8)$$

where $\Omega_d = (g\mu_B S)^2 N/V$ measures the strength of the dipolar interaction. Footing on numerous results from neutron scattering, the correlation functions $C_\alpha(q,t) = (S_\alpha(\mathbf{q},t)S_\alpha(\mathbf{q},0))$ of the transverse ($\alpha = t$)[16,17,40] and longitudinal ($\alpha = \ell$) [18] modes are taken to decay exponentially, $C_\alpha(\mathbf{q},t) = C_\alpha(\mathbf{q})exp(-\Gamma_\alpha(\mathbf{q})t)$, so that one finds [11,20]:

$$\tilde{L}_z(\omega) = \Omega_d^2 \quad \sum_{\mathbf{q}} \frac{C_\ell(\mathbf{q})C_t(\mathbf{q})}{\Gamma_\ell(\mathbf{q}) + \Gamma_t(\mathbf{q}) + i\omega}\,. \qquad (9)$$

Near the Curie temperature, the sum is heavily weighted by C_t due to the divergence of $\chi_t(\mathbf{q} \to 0) = (q_d\xi)^2$, whereas $C_\ell \to 1$ saturates in this limit [34]. This criticality of the transverse modes leads to the slowing down of their relaxation rates,

$$\Gamma_t(\mathbf{q} \to 0, T \geq T_c) = A\ q^{5/2}\gamma_t(q\xi(T)), \qquad (10)$$

where $\gamma_t(x)$ is a homogeneous (scaling) function with $\gamma_t(x \to \infty) \to 1$ [19]. On the other hand, the relaxation rate of the noncritical longitudinal modes saturates near T_c for $q < q_d$:

$$\Gamma_\ell \equiv \Gamma_\ell(q < q_d, T \to T_c) = A\ q_d^{5/2}. \qquad (11)$$

The nonuniversal parameter A entering both, Γ_ℓ and Γ_t, can be expressed by T_c and by the dipolar wavenumber q_d [6,19], $A \approx \gamma(k_B T_c/\mu_0)^{1/2}/q_d$, where $\gamma = g\mu_B/\hbar$ denotes the gyromagnetic ratio. It was shown earlier [6] for many archetype Heisenberg ferromagnets including EuS and EuO, that A describes the existing experimental data for $\Gamma_t(\mathbf{q} \to 0)$ obtained by inelastic neutron scattering rather accurately. More recently, also the relaxation rate of the longitudinal spin fluctuations has been measured by inelastic scattering of polarized neutrons [18] on EuS, and the result $\Gamma_\ell(\mathbf{q} \to 0, T \to T_c) = 0.98(15) \times 10^{11}$ s^{-1} was found to agree with the prediction by equation (11).

Taking all these observations into account, the summation in equation (9) leads to [11,20]

$$\tilde{L}_z^{MC}(\omega;\chi_z) = \frac{1}{[1+\chi_z^{-1}]^{7/4}} \cdot \frac{L_z^{MC}(T_c,0)}{1+i\omega/\Gamma_\ell} \qquad (12)$$

with $L_z^{MC}(T_c,0) \simeq A\ q_d^{5/2}$ [6]. It is now interesting to note that this frequency variation, which should strictly be valid only at zero magnetization, corresponds to our experimental result, equation (6), obtained for temperatures $T \leq T_c$. This implies that the experimental correlation frequency has to be identified with the relaxation rate of the longitudinal fluctuations, and in fact the value for EuS emerging from this work, $\omega_c = 1.2(4) \times 10^{11}$ s^{-1}, excellently agrees with $\Gamma_\ell = 0.98(15) \times 10^{11}$ s^{-1}. Our value for EuO, $\omega_c = 1.0(3) \times 10^{11}$ s^{-1}, can quantitatively be explained in terms of equations (10) and (11), which give $\Gamma_\ell = \Gamma_t(q_d/q)^{5/2} = 1.13 \times 10^{11}$ s^{-1}, by using Γ_t from neutron scattering and $q_d = 0.15$ Å^{-1} [6,16]. Thus we can conclude that *the fast relaxation of the longitudinal modes does govern the homogeneous dynamics not only above T_c but also in the wide region below T_c examined here.*

The other significant feature indicating the importance of the longitudinal fluctuations below T_c is the scaling behavior of the kinetic coefficient, $L_z(T,H)$, evidenced in Figure 5. For both ferromagnets, the scaling functions can be well described by the dc-limit of equation (12), $\tilde{L}_z(0,\chi_z(T,H)) = L_z(T_c,0)/[1+\chi_z^{-1}(T,H)]^{7/4}$, which was derived for zero magnetization, $M_z = 0$ [19]. Let us mention that equation (12) also explains the result of a previous, preliminary study near the coexistence line of EuS [7], where, $\tilde{L}_z(0, T \leq T_c, H \to 0)$ was found to remain constant. Obviously, this arises from the divergence of χ_z at the coexistence line, see Figure 5.

If a finite magnetization is present, the evaluation of L_z from equation (7) involves modes parallel and perpendicular to M_z. Due to the dipolar interaction these parallel and spin-wave modes are further split into longitudinal and transverse ones. The high complexity of the resulting problem has been realized already by Vaks *et al.* [41]. Very recently, Schinz and Schwabl [42] investigated in more detail the dipolar effects on spin-wave frequencies and linewidths, however, the dynamics of the parallel fluctuations is still waiting for a solution. Regarding our main observations, *i.e.* the memory effect and the scaling property of L_z, we suspect here that below T_c (i) the damping of $\delta S_z(q_t = 0)$ is determined primarily by the transverse and longitudinal modes of the parallel magnetization, $\delta S_z(\mathbf{q}\perp\mathbf{e_z})$ and $\delta S_z(\mathbf{q} \parallel \mathbf{e_z})$, and (ii) that the coupling of $\delta S_z(\mathbf{q})$ to the spin-waves $\delta S_{SW}(\mathbf{q})$ seems to be of minor importance here. Of course, a direct proof of this conjecture *e.g.* by neutron scattering would be of great value.

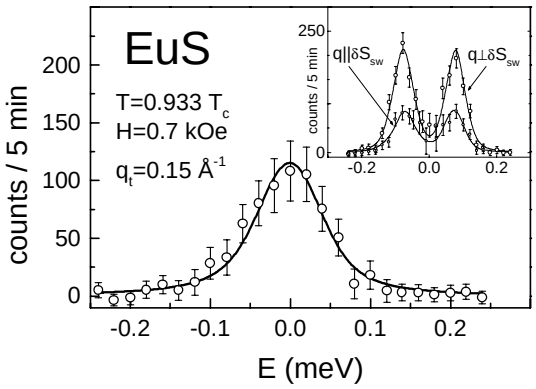

Fig. 7. Neutron scattering from the transverse ($\mathbf{q}\perp\mathbf{M}$) parallel magnetization fluctuations below T_c at the internal field $H = 0.7$ kOe. The inset shows the results from the transverse and longitudinal spin-wave fluctuations.

A first step in this direction has been made very recently on EuS, where the dynamics of the spin-wave and the parallel fluctuations (see Fig. 4b) has been measured separately using inelastic scattering of polarized neutrons [24]. Two spectra are reproduced in Figure 7 showing a pure relaxational peak for the transverse, parallel fluctuations, as opposed to the two propagating, *i.e.* longitudinal and transverse spin-wave modes shown by the inset. The analysis of the linewidth yields $\Gamma_z(q_t) = 20(1)$ μeV and the energy integration of the peak yields for the susceptibility $\chi_z(\mathbf{q}_t) = 0.68(2)$ at the temperature and the internal field given in Figure 7. Indicating the value for the susceptibility in Figure 3a we find an excellent agreement with our results for $\chi_z(\mathbf{q}_t = 0)$. Without having any detailed knowledge on the $\mathbf{q}$-variation of χ_z we can only speculate that this finding arises from the fact that q_t is significantly smaller than the the dipolar wavenumber $q_d = 0.24$ Å^{-1}, so that χ_z may saturate.

The evaluation of the kinetic coefficient by using these numbers gives $L_z(q_t) \equiv \Gamma_z(q_t)\chi_z(q_t) = 3.1(8) \times 10^{10}$ s^{-1}. This result does not hit exactly the scaling curve of Figure 5a for the homogeneous kinetic coefficient. This shows that the dynamic quantity L_z may be more sensitive against a variation of q_t in the dipolar regime $q < q_d$ than the static susceptibility. However, the closeness of $L_z(q_t = 0.69q_d)$ to $L_z(0)$ indicates that this effect is not very strong.

6 Summary and conclusions

The effects of temperature and magnetic fields on the static and dynamic susceptibilities have been investigated in the domain free states below the Curie temperatures of the weakly anisotropic Heisenberg ferromagnets EuS and EuO. We have shown that the dipolar anisotropic spin-wave fluctuations dominate the static susceptibility $\chi_z(0)$ of the homogeneous magnetization not only for $T \ll T_c$ but also for temperatures very close to the Curie points. It was exemplified for EuO that the cubic anisotropy has no impact on $\chi_z(0)$ for fields exceeding the anisotropy field $H_A(T)$.

The dynamic susceptibilities exhibit a heavily damped Lorentzian. This shape is related to a memory effect: a Debye function for the damping $L_z(\omega)$ containing a field and temperature independent correlation frequency ω_c completely describes the oscillatory behavior of $\chi_{zz}(\omega)$ below T_c. By extending the MC work of Frey and Schwabl [19,20] for Heisenberg ferromagnets with dipolar interaction to finite frequencies at $T \leq T_c$, ω_c is identified with the relaxation rate Γ_ℓ of the longitudinal fluctuations of the small wavenumber ($q < q_d$) modes parallel to the magnetization M_z. The kinetic coefficients of the damping $L_z(\omega \to 0; T, H)$ scale with $\chi_z(T, H)$ on master curves which are identical (i) to the scaling function previously determined above T_c of EuS and (ii) to a prediction of the MC-work for the paramagnetic critical regime [19,20]. These two features suggest that also below T_c the anisotropic dipolar fluctuations dominate the homogeneous magnetization dynamics and that this novel feature calls for a more detailed explanation.

The authors thank R. Dombrowski and A. Flossdorff (both Hamburg) for the help during the microwave measurements and M. Baumann (Hamburg), who supplied the magnetization data on the samples. The collaboration with P. Böni (PSI Villigen) during the neutron scattering work is highly appreciated.

References

1. J. Kötzler, G. Kamleiter, G. Weber, J. Phys. C: Solid State Phys. **9**, L361 (1976).
2. L.J. de Haas, J.C. Verstelle, Physica B **86-88**, 1291 (1977).
3. J. Kötzler, H.V. Philipsborn, Phys. Rev. Lett. **40**, 790 (1978).
4. M. Shini, T. Hashimoto, Phys. Lett. A **68**, 241 (1978).
5. R.A. Dunlap, A.M. Gottlieb, Phys. Rev. B **22**, 3422 (1980).
6. J. Kötzler, Phys. Rev. B **38**, 12027 (1988).
7. J. Kötzler, E. Kaldis, G. Kamleiter, G. Weber, Phys. Rev. B **43**, 11280 (1991).
8. M. Grahl *et al.*, J. Appl. Phys. **69**, 6179 (1991).
9. D. Görlitz, J. Kötzler, T. Lange, J. Magn. Magn. Mat. **104-107**, 339 (1992).
10. R. Dombrowski, D. Görlitz, J. Kötzler, C. Marx, J. Appl. Phys. **75**, 6054 (1994).
11. J. Kötzler, D. Görlitz, M. Hartl, C. Marx, IEEE - MAG. **30**, 828 (1994).
12. A. Flosdorff, D. Görlitz, J. Kötzler, J. Appl. Phys. **79**, 4641 (1996).
13. J. Kötzler, Phys. Rev. Lett. **51**, 833 (1983).
14. F. Mezei, Phys. Rev. Lett. **49**, 1096, 1537(E) (1982).
15. L. Passell, O.W. Dietrich, J. Als-Nielsen, Phys. Rev. B **14**, 4897 (1976).
16. F. Mezei, Physica B **136**, 417 (1986).
17. P. Böni, G. Shirane, H.G. Bohn, W. Zinn, J. Appl. Phys. **63**, 3089 (1988).
18. P. Böni, D. Görlitz, J. Kötzler, J.L. Martínez, Phys. Rev. B **43**, R8755 (1991).

19. E. Frey, F. Schwabl, Z. Phys. B **71**, 355 (1988).
20. E. Frey, F. Schwabl, Adv. Phys. **43**, 577 (1994).
21. J. Kötzler, D. Görlitz, R. Dombrowski, M. Pieper, Z. Phys. B **94**, 9 (1994).
22. T. Holstein, H. Primakoff, Phys. Rev. **58**, 1098 (1940).
23. V.L. Prokrovsky, Adv. Phys. **28**, 595 (1979).
24. P. Böni *et al.*, Proc. IAEA TCM *Neutron Beam Research*, ITN, Lisbon 68 (1997).
25. D. Görlitz, J. Kapoor, J. Kötzler, J. Phys. E **22**, 884 (1989).
26. The internal fields H were obtained from SQUID magnetizations $M_z(T, H)$, measurements by M. Baumann (unpublished).
27. W. Finger, Physica B **90**, 251 (1977).
28. F. Schwabl, K.H. Michel, Phys. Rev. B **2**, 189 (1970).
29. M.E. Fisher, V. Privman, Phys. Rev. B **32**, 447 (1985).
30. H.S. Toh, G.A. Gehring, J. Phys.: Cond. Mat. **2**, 7511 (1990).
31. S.W. Lovesey, K. Trohidou, J. Phys.: Cond. Mat. **3**, 1827 (1991).
32. R. Arias, H. Suhl, Phys. Rev. B **51**, 979 (1995).
33. D.A. Garanin, Z. Phys. B **102**, 283 (1997).
34. J. Kötzler, F. Mezei, D. Görlitz, B. Farago, Europhys. Lett. **1**, 675 (1986).
35. J.J.F. Dillon, C.E. Olson, Phys. Rev. **135**, A434 (1964).
36. M.C. Franzblau, G.E. Everett, A.W. Lawson, Phys. Rev. **164**, 716 (1967).
37. D.L. Huber, J. Phys. Chem. Solids **32**, 2145 (1971).
38. R. Raghavan, D.L. Huber, Phys. Rev. B **14**, 1185 (1976).
39. S.V. Maleev, Soc. Sci. Rev. A. Phys. **8**, 323 (1987).
40. O.W. Dietrich, J. Als-Nielsen, L. Passell, Phys. Rev. B **14**, 4923 (1976).
41. V.G. Vaks, A.I. Larkin, S.A. Pikin, Soviet Phys.- JETP **26**, 188 (1968).
42. H. Schinz, F. Schwabl, Phys. Rev. B **57**, 8438 (1998).